Synchronization of chaotic networks with time-delayed couplings: An analytic study

A. Englert,[1] S. Heiligenthal,[1] W. Kinzel,[1] and I. Kanter[2]
[1]*Institute for Theoretical Physics, University of Würzburg, D-97074 Würzburg, Germany*
[2]*Department of Physics, Bar-Ilan University, Ramat-Gan, IL-52900 Israel*
(Received 20 January 2011; published 26 April 2011)

Networks of nonlinear units with time-delayed couplings can synchronize to a common chaotic trajectory. Although the delay time may be very large, the units can synchronize completely without time shift. For networks of coupled Bernoulli maps, analytic results are derived for the stability of the chaotic synchronization manifold. For a single delay time, chaos synchronization is related to the spectral gap of the coupling matrix. For networks with multiple delay times, analytic results are obtained from the theory of polynomials. Finally, the analytic results are compared with networks of iterated tent maps and Lang-Kobayashi equations, which imitate the behavior of networks of semiconductor lasers.

DOI: 10.1103/PhysRevE.83.046222 PACS number(s): 05.45.Xt, 05.45.Pq, 05.10.−a

I. INTRODUCTION

Chaos synchronization is a phenomenon which is of fundamental scientific interest in nonlinear dynamics and which is being investigated in the context of secure communication and neural activity [1–5]. In particular, networks of nonlinear units which relax to a common chaotic trajectory are the focus of recent research [6,7].

For many applications, the coupling between nonlinear dynamical units is realized by transmitting a function of their internal variables to their neighbors. In many cases, the transmission time is larger than the internal time scales of the units. One example are chaotic lasers which are coupled by their mutual laser beams [5,8–11]. Thus, networks of nonlinear units which are coupled by their time-delayed variables—including time-delayed self-feedback—are a subject of recent research activities [6,12–32].

The theoretical investigations of chaotic networks are mainly based on numerical simulations. However, there exists a powerful method to determine the stability of the synchronization manifold (SM) of an *arbitrary* network: the master stability function (MSF) [29]. This method connects topology with function. Using the eigenvalues of the connection matrix, a linear equation for a *single* unit is derived which determines the stability of chaos synchronization for the *complete* network. For the case of time-delayed couplings, the MSF has been studied for few systems only [20,25,33].

The MSF is defined as the maximal Lyapunov exponent of linear equations with time-dependent coefficients. In general, it is not possible to derive analytic results for these equations because the coefficients are given by the chaotic trajectory of the network. Thus, one has to rely on numerical simulations of the linear system of differential equations (for chaotic flows) or difference equations (for coupled map lattices).

The purpose of this paper is to derive analytic results for chaotic networks with time-delayed couplings. Thus, we concentrate on a coupled map lattice, a network of chaotic iterated Bernoulli maps, which allows an analytic calculation of the MSF. The corresponding linear difference equations have constant coefficients. Therefore, stability of the solution is related to the roots of polynomials. Results from graph theory, control theory, and algebra will help to derive analytic statements about chaos synchronization.

The linear stability equations of Bernoulli networks may be considered as approximations for linear equations with time-dependent couplings. Thus, we compare our analytic results with numerical results for other iterated maps and with simulations of rate equations for coupled semiconductor lasers. In the following section, the MSF for chaotic networks with time-delayed couplings is introduced. We concentrate on networks where chaos is generated by the couplings and/or self-feedback, similar to semiconductor lasers. Afterward, analytic results are derived for Bernoulli networks with single and multiple delay times. The last section compares these results with networks of iterated tent maps and networks of laser rate equations.

II. MASTER STABILITY FUNCTION (MSF)

A. MSF with time delay

One powerful method to analyze the stability of synchronization in networks of coupled systems with identical units is the MSF proposed by Pecora and Caroll [29]. A network of coupled identical dynamical units can be analyzed by linearizing the dynamical equation around the synchronization manifold.

In order to obtain analytic results, we restrict our investigation to coupled map lattices, and we use an identical function $f(x)$, $x \in [0,1]$ for the internal dynamic, the self-feedback, and the couplings. We extend the master stability function of [29] for a system without time delay to a system with arbitrarily many different time delays [27,34–36], where each term with delay time τ_l is weighted with a positive coupling parameter σ_l and a positive self-feedback parameter η_l. The network consists of N units with variables $x_t^i \in [0,1]$, where $i = 1,\ldots,N$ is the index of the unit and t is a discrete time step. The system is defined by

$$x_t^i = \eta_0 f\left(x_{t-1}^i\right) + \sum_{l=1}^{M} \eta_l \, f\left(x_{t-\tau_l}^i\right) + \sum_{l=1}^{M}\sum_{j=1}^{N} \sigma_l \, G_{l,ij} \, f\left(x_{t-\tau_l}^j\right). \tag{1}$$

Without loss of generality, we order the coupling terms with ascending delay times, so that τ_M is the maximum time delay. Each coupling delay time τ_l has its own coupling matrix, the

normalized weighted adjacency matrix G_l with $\sum_j G_{l,ij} = 1$ and $G_{ij} \geqslant 0$ [24,31]. Therefore, the coupling is invasive and nondiffusive; it changes the trajectory of the coupled system in comparison to a noncoupled system. We assume that the coupling matrices G_l commute; otherwise, the MSF method cannot be applied. The self-feedback of the system is not included in G_l; hence $G_{l,ii} = 0$.

Complete zero-lag synchronization $x_t^1 = \cdots = x_t^N = s_t$ is a solution of these equations. The synchronized trajectory is given by

$$s_t = \eta_0 \, f(s_{t-1}) + \sum_{l=1}^{M} (\eta_l + \sigma_l) f(s_{t-\tau_l}). \tag{2}$$

The stability of the SM is determined by linearizing Eq. (1) in the vicinity of the SM, Eq. (2). With $\delta x_t^i = x_t^i - s_t$, we obtain

$$\delta x_t^i = \eta_0 \, f'(s_{t-1}) \delta x_{t-1}^i + \sum_{l=1}^{M} \eta_l \, f'(s_{t-\tau_l}) \delta x_{t-\tau_l}^i + \sum_{l=1}^{M} \sum_{j=1}^{N} \sigma_l \, G_{l,ij} \, f'(s_{t-\tau_l}) \delta x_{t-\tau_l}^j. \tag{3}$$

For a network with N nodes, we obtain N coupled linear equations with time-dependent coefficients. Since the coupling matrices G_l commute, we can expand the N-dimensional perturbation $\delta \vec{x}_t$ to the common eigenvectors $\vec{w}_k$ with eigenvalues $\gamma_{l,k}$, $k = 1, \ldots, N$, $l = 1, \ldots, M$ of the matrices G_l. For each mode k of the perturbation, with $\delta \vec{x}_t = \xi_{k,t} \, \vec{w}_k$, we obtain

$$\xi_{k,t} = \sum_{l=0}^{M} (\eta_l + \sigma_l \, \gamma_{k,l}) f'(s_{t-\tau_l}) \xi_{k,t-\tau_l}, \tag{4}$$

where we have defined $\sigma_0 = 0$ and $\tau_0 = 1$. $\xi_{k,t}$ is the amplitude of the perturbation corresponding to the eigenvalue $\gamma_{k,l}$ of the coupling matrix G_l.

To gain analytic results, we focus on a chaotic map with constant slope, namely the Bernoulli map, which is given by

$$f(x) = (\alpha \, x) \bmod 1 \tag{5}$$

and is chaotic for $\alpha > 1$. Since $f'(s_t) = \alpha$ is constant, Eq. (4) becomes

$$\xi_{k,t} = \sum_{l=0}^{M} (\eta_l + \sigma_l \, \gamma_{k,l}) \alpha \, \xi_{k,t-\tau_l}. \tag{6}$$

With the ansatz $\xi_{k,t} = z_k^t \, \xi_{k,0}$, the whole stability problem becomes a problem of solving the polynomial of degree τ_M,

$$z_k^{\tau_M} = \sum_{l=0}^{M} (\eta_l + \sigma_l \, \gamma_{k,l}) \alpha \, z_k^{\tau_M - \tau_l} = \sum_{l=0}^{M} \beta_{k,l} \, z_k^{\tau_M - \tau_l}, \tag{7}$$

with $\beta_{k,l} = (\eta_l + \sigma_l \, \gamma_{k,l}) \alpha$.

For each eigenvalue γ_k, Eq. (7) yields τ_M roots, which we label with $z_{k,r}$ with $r = 1, \ldots, \tau_M$. Our goal is to find coupling parameters $\beta_{k,l}$ such that the following points are true:

(1) For $\gamma_{0,l} = 1, l = 1, \ldots, M$, there exists at least one z_{0,r_m} and $|z_{0,r_m}| > 1$. This guarantees a chaotic dynamic of the SM.

(2) For each $\gamma_k (k > 1)$, all roots $z_{k,r}$ lie inside the unit circle $|z_{k,r}| < 1$. This guarantees a stable SM. In this case, the MSF is defined as

$$\lambda = \max_{k>0,r} \ln |z_{k,r}|. \tag{8}$$

Equation (7) allows an analytic investigation of chaos synchronization. Later, we discuss to what extent Eq. (7) is a good approximation for other iterated maps with time-dependent slopes f' and even for corresponding differential equations with time-dependent Jacobi matrices.

B. Concept of local Lyapunov exponents

The stability of the SM of the complete network is determined by the linear equation (4). This equation yields the Lyapunov exponents of the network parallel ($\gamma_0 = 1$) and perpendicular (γ_k, $k > 0$) to the SM. As we see later, it is useful to consider the contributions of individual terms in Eq. (4) to the stability of the SM separately. Hence, we define "local Lyapunov exponents" to discuss these contributions. For example, the local Lyapunov exponent is defined as the maximal one of the equation

$$\xi_{k,t} = \eta_0 \, f'(s_{t-1}) \xi_{k,t-1}, \tag{9}$$

where s_t is the trajectory of the complete network, including time-delayed terms.

For the case of large delay times τ_l, one finds the following result: When the instantaneous Lyapunov exponent is positive, the network cannot synchronize [25]. Note that local Lyapunov exponents are not the Lyapunov exponents of the isolated units, since the network changes the trajectory. Only for the Bernoulli network, the linear equations do not depend on the trajectory; in this case, the local Lyapunov exponents are identical to the ones of the corresponding isolated units.

C. Graph spectrum

The stability of the SM is determined by the eigenvalues of the coupling matrices G_l, according to the MSF Eq. (8). We consider matrices with unit row sum, $\sum_j G_{l,ij} = 1$. Since we consider self-feedback separately, we have $G_{l,ii} = 0$.

We restrict our discussion to non-negative matrices [37], $G_{l,ij} \geqslant 0$, and to completely connected graphs. One eigenvalue is unity, $\gamma_{0,l} = 1$, and according to the Perron-Frobenius theorem $\gamma_{0,l}$ is not degenerate and has the largest modulus of all eigenvalues of G_l. Therefore, we order the eigenvalues such that $1 = \gamma_{0,l} \geqslant |\gamma_{1,l}| \geqslant |\gamma_{2,l}| \geqslant \cdots \geqslant |\gamma_{N-1,l}|$.

The eigenvector for the largest eigenvalue $\gamma_0 = 1$ is $\vec{w}_0 = (1, \ldots, 1)$. It corresponds to a perturbation parallel to the SM. Since we discuss only chaotic networks, the Lyapunov exponent $\lambda_{\max}$ of the mode γ_0 is positive; the dynamics in the SM, Eq. (2), is chaotic. As we show later, for large single delay time τ, the spectral gap $\Delta = 1 - |\gamma_1|$ determines the stability of the SM. Complete zero-lag synchronization is possible in the limit of weak chaos, $\lambda_{\max} \to 0$, if and only if the spectral gap is nonzero, $|\gamma_1| < 1$.

The theory of non-negative matrices [37] relates the eigenvalue gap to the loop structure of the corresponding graph: Δ is nonzero if and only if the greatest common divisor of the length of loops of the graph is unity. Hence, for a

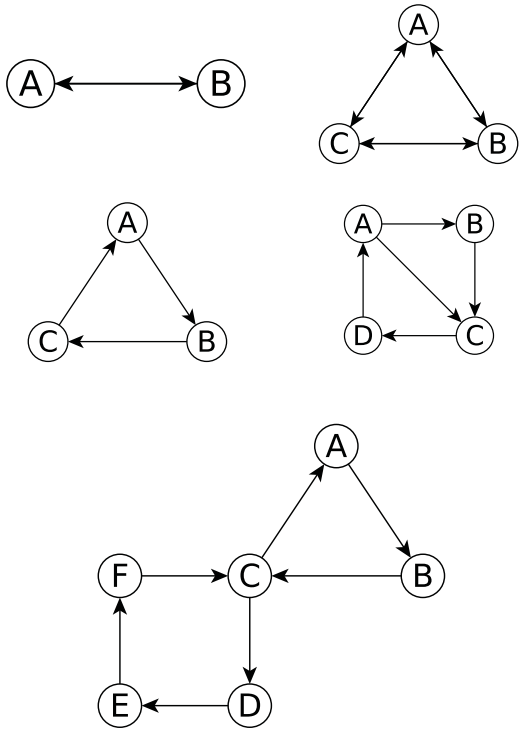

FIG. 1. Schemata of bidirectionally coupled pair, spectral gap $\Delta = 0$; bidirectionally coupled triangle, $\Delta = \frac{1}{2}$; unidirectional triangle, $\Delta = 0$; square, $\Delta = 0.1215$; and combination of triangle and square, $\Delta = 0.1215$. These are the values for equal coupling weights.

single large time delay, it is easy to see whether a network can synchronize in the limit of weak chaos. In fact, this result has been extended to networks with multiple delay times τ_l by a self-consistent physical argument based on mixing information of the chaotic trajectories of the nodes [23].

For some single graphs, the eigenvalues are known analytically. Figure 1 shows the eigenvalue gap for some graphs. Note that a directed triangle and a directed square have zero gaps, but if one connects them, the greatest common divisor of loops 3 and 4 is unity and the gap is nonzero [37].

III. ANALYTIC RESULTS

In this section, we present analytic results for Bernoulli networks. We focus on complete zero-lag synchronization. According to the previous section, the stability of the SM is determined by the roots of the following polynomials:

$$z^{\tau_M} = \sum_{l=0}^{M} (\eta_l + \sigma_l \gamma_{k,l})\alpha \, z^{\tau_M - \tau_l} = \sum_{l=0}^{M} \beta_l \, z^{\tau_M - \tau_l}. \quad (10)$$

Note that each β_l includes $\gamma_{k,l}$ and that we omitted the index k in our notation.

The network contains $M+1$ different delay times τ_l, and τ_M is the largest one. For each mode k of perturbation, we have a set of eigenvalues $\gamma_{k,l}$ of the coupling matrices G_l corresponding to the delay times τ_l. Hence, we have to calculate the roots of Eq. (10) with $\beta_l = (\eta_l + \sigma_l \gamma_{k,l})\alpha$ for each mode of perturbation, where σ_l is the coupling strength and α is the slope of the Bernoulli map. Equation (10) includes the local dynamics with $\tau_0 = 1$ and $\sigma_0 = 0$ and self-feedbacks with delay time τ_l and strength η_l. The mode parallel to the SM has eigenvalues $\gamma_{0,l} = 1$ for all terms of Eq. (10).

Some results can be derived immediately. The polynomial Eq. (10) has τ_M roots z_r and the theorem of Vieta gives $\prod_r |z_r| = |\beta_M|$. Hence, for $|\beta_M| > 1$, at least one root is outside of the unit circle. Consequently, all modes k with $|(\eta_M + \sigma_M \gamma_{k,M})\alpha| > 1$ are unstable. If the coupling σ_M and the self-feedback η_M of the largest delay time τ_M are such that there exists one eigenvalue $\gamma_{k,M}$ with $k > 0$ and $|\eta_M + \sigma_M \gamma_{k,M}| > 1/\alpha$, the network cannot synchronize and the SM is unstable.

Equation (10) denotes the roots of a polynomial $P(z)$, which can be written as

$$P(z) = z^{\tau_M} - \sum_{l=0}^{M} (\eta_l + \sigma_l \gamma_{k,l})\alpha \, z^{\tau_M - \tau_l}. \quad (11)$$

If the mode k is unstable, $P(z)$ has at least one root with $|z| > 1$. Let us assume $\sum_{l=0}^{M} (\eta_l + \sigma_l \gamma_{k,l})\alpha > 1$, which gives

$$P(1) = 1 - \sum_{l=0}^{M} (\eta_l + \sigma_l \gamma_{k,l})\alpha < 0. \quad (12)$$

Furthermore, on the real axis we have

$$\lim_{z \to \infty} P(z) \to \infty. \quad (13)$$

Since $P(z)$ is continuous, we can conclude that $P(z)$ has a root on the real axis with $z_0 > 1$. Hence, the mode k is unstable if

$$\sum_{l=0}^{M} (\eta_l + \sigma_l \gamma_{k,l})\alpha > 1. \quad (14)$$

Gershgorin's circle theorem [38] states that all roots of $P(z)$ lie inside a circle with radius R given by the inequality

$$R \leqslant \max \left\{ 1, \sum_{l=0}^{M} |(\eta_l + \sigma_l \gamma_{k,l})\alpha| \right\}, \quad (15)$$

Hence, the mode k is stable if

$$\sum_{l=0}^{M} |(\eta_l + \sigma_l \gamma_{k,l})\alpha| < 1. \quad (16)$$

Equations (14) and (16) give the parameter regime for chaos. Note that this is valid for all perturbation modes k.

For a chaotic trajectory, the perturbation mode parallel to the synchronization manifold, $\gamma_{0,l} = 1$, has to be unstable. This is the case for

$$\sum_{l=0}^{M} (\eta_l + \sigma_l)\alpha > 1, \quad (17)$$

whereas for

$$\sum_{l=0}^{M} (\eta_l + \sigma_l)\alpha < 1 \quad (18)$$

the perturbation mode for $k = 0$ is stable. Hence, the border to a chaotic trajectory is given by

$$1 = \sum_{l=0}^{M} \beta_l = \sum_{l=0}^{M} (\eta_l + \sigma_l)\alpha. \quad (19)$$

If the sum of couplings is larger than 1, the system is chaotic. Note that this transition to chaos does not depend on the delay times τ_l, in contrast to the region of synchronization, which is very sensitive to the values of the delay times τ_l. In this work, we consider only parameters where the network is chaotic. Another conclusion from this result is the fact that for some networks it is always possible to find coupling parameters and Bernoulli slopes for which stable chaos synchronization is possible. This networks have to have eigenvalues $k > 0$, which fulfill Eq. (16) for parameters, which ensure Eq. (17). This is the case for $|\gamma_{k,l}| < 1$, where $k > 0$.

A. Single delay time

For a network with a single delay time τ, including coupling and self-feedback, we have to find the roots of

$$z^\tau = \beta_0 z^{\tau-1} + \beta_1 = \eta_0 \alpha z^{\tau-1} + (\eta_1 + \sigma_1 \gamma_k)\alpha \qquad (20)$$

in the chaotic region

$$(\eta_0 + \eta_1 + \sigma_1)\alpha > 1. \qquad (21)$$

For each mode k, Eq. (20) has τ roots $z_{k,r}$, which define a spectrum of τ Lyapunov exponents $\lambda_{k,r} = \ln|z_{k,r}|$. Figure 2 shows this spectrum as a function of the parameters β_0 and β_1. For $\beta_0 + \beta_1 > 0$, the maximal Lyapunov exponent is positive. Using the Schur-Cohn theorem [39], the region of stability can be calculated numerically. Figure 3 shows the results for $\tau = 2{,}4$ and $\tau \to \infty$. With increasing delay time, this region shrinks to the symmetric triangle $|\beta_1| < 1 - \beta_0$.

In fact, one can derive the region of stability analytically for $\tau \to \infty$. In this limit, we have to consider two cases: (a) the Lyapunov exponent is of order 1 and (b) it is of order $1/\tau$ [40,41]. We omit the index k of the root $z_{k,r}$ of the perturbation mode k since γ_k is included in β_1. From Eq. (20), we obtain

$$|z_r|^\tau = \left|\frac{\beta_1 z_r}{z_r - \beta_0}\right|. \qquad (22)$$

For case (a), $|z_r|^\tau$ diverges for $\tau \to \infty$ in the region of instability, and hence we find $z_r = \beta_0$ for $\tau \to \infty$. If $\beta_0 > 1$, the SM is unstable for any perturbation mode with eigenvalue γ_k. However, $\beta_0 > 1$ means that the uncoupled units are chaotic. Thus, we reproduce the result already found in [25]: If the local Lyapunov exponent defined in the previous section is positive, a network cannot be synchronized by time-delayed couplings if the delay time is much larger than the local time scales.

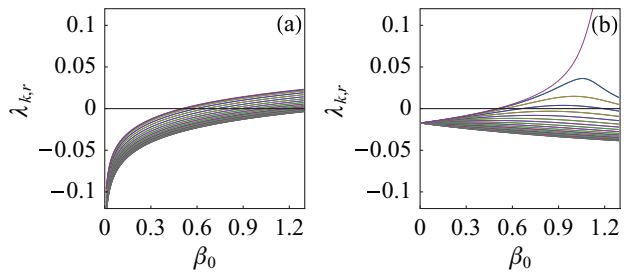

FIG. 2. (Color online) Spectrum of Lyapunov exponents for the system of Eq. (20) and $\tau = 40$. (a) $\beta_0 = 0.5$ and (b) $\beta_1 = 0.5$. There is at least one positive Lyapunov exponent for $\beta_0 + \beta_1 \geqslant 1$.

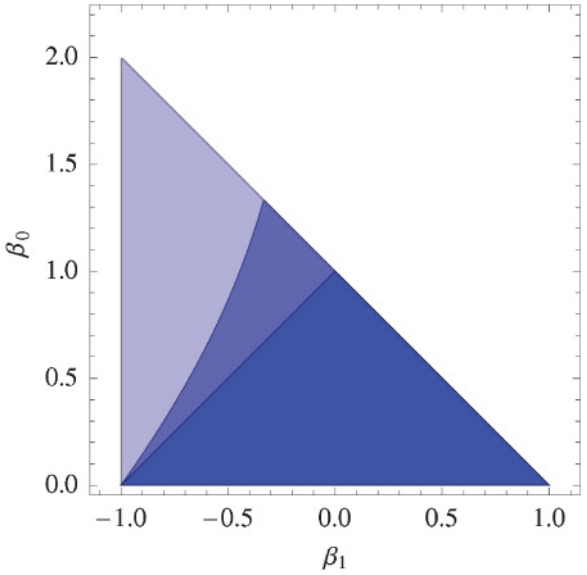

FIG. 3. (Color online) Synchronization regime for $z^\tau = \beta_0 z^{\tau-1} + \beta_1$ and $\tau = 2$ (light blue), $\tau = 4$ (medium blue), and $\tau \to \infty$ (dark blue). Note that $\tau \to \infty$ regime is a subset of $\tau = 2$ and $\tau = 4$ regime and that $\tau = 4$ regime is a subset of $\tau = 2$ regime.

For case (b), we write $z_r = e^{\lambda_r} e^{i\phi_r}$ with $\lambda_r = \Lambda_r/\tau$. Equation (22) gives

$$e^{\Lambda_r} = \frac{|\beta_1| e^{\Lambda_r/\tau}}{|e^{\Lambda_r/\tau} e^{i\phi_r} - \beta_0|}. \qquad (23)$$

For $\tau \to \infty$, we obtain

$$e^{2\Lambda_r} = \frac{|\beta_1|^2}{\beta_0^2 - 2\beta_0 \cos\phi_r + 1}. \qquad (24)$$

For $\tau \to \infty$, the phases ϕ_r are uniformly distributed on the circle $[0,2\pi]$ [42,43], and hence the maximal Lyapunov exponent is given for $\phi_r = 0$, which yields the region of stability

$$|\beta_1| < 1 - \beta_0. \qquad (25)$$

Consequently, the network can synchronize if for all $k > 0$

$$|(\eta_1 + \sigma_1 \gamma_k)\alpha| < 1 - \eta_0 \alpha. \qquad (26)$$

For large delay times and without self-feedback $\eta_1 = 0$, Eq. (26) reduces to

$$|\sigma_1 \gamma_1 \alpha| < 1 - \eta_0 \alpha, \qquad (27)$$

where γ_1 is the eigenvalue with the second largest absolute value, $1 \geqslant |\gamma_1| \geqslant |\gamma_2| \ldots$. Neither the sign nor the complex phase of the eigenvalue γ_1 have an influence on the region of stability. This is different for small values of τ where the region of stability depends on the complex phase of γ_1. Note that this symmetry for large delay times has recently been proven for general chaotic networks with a continuous dynamics [30]. Equation (27) has interesting consequences. The network is chaotic if

$$\sigma_1 \alpha > 1 - \eta_0 \alpha. \qquad (28)$$

It can synchronize if

$$\sigma_0\,\alpha + |\sigma_1\,\gamma_1\,\alpha| < 1. \tag{29}$$

Thus, if $|\gamma_1| = 1$, Eq. (27) is identical to Eq. (28) and the chaotic network cannot synchronize for any set of parameters. For bipartite networks, one finds $\gamma_1 = -1$, hence bipartite networks cannot synchronize completely; only sublattice or cluster synchronization is possible [24,31]. According to Fig. 1, a pair, a square without diagonals, or any directed ring cannot synchronize completely for large delay times. A sublattice or cluster synchronization, however, is possible [23,24,31]. On the other hand, a triangle with bidirectional couplings can synchronize completely, since $\gamma_1 = -\frac{1}{2}$.

We exemplify this result by a system consisting of two bidirectionally coupled Bernoulli units with one time delay τ for the coupling and the same time delay τ for self-feedback. By adding a self-feedback with delay time τ, one can achieve complete synchronization in a bidirectionally coupled pair. The dynamical equation of unit i is defined as

$$x_t^i = (1-\varepsilon)\,f\big(x_t^i\big) + \varepsilon\,\kappa\,f\big(x_{t-\tau}^i\big) + \varepsilon\,(1-\kappa)\,f\big(x_{t-\tau}^j\big), \tag{30}$$

with $i,j \in \{1,2\}$. According to Eq. (28), the system is chaotic for any parameters $f'(x) = \alpha > 1$ and $\varepsilon,\kappa \in [0,1]$. The pair has the eigenvalue $\gamma_1 = -1$, which gives $\beta_0 = (1-\varepsilon)\,\alpha$, $\beta_1 = \varepsilon\,(2\,\kappa - 1)\,\alpha$. Equation (25) yields two synchronization borders for $\tau \to \infty$:

$$\kappa^+(\varepsilon) = 1 - \frac{\alpha - 1}{2\,\alpha\,\varepsilon},$$
$$\kappa^-(\varepsilon) = \frac{\alpha - 1}{2\,\alpha\,\varepsilon}. \tag{31}$$

For a triangle with corresponding equations, we obtain with $\gamma_1 = -\frac{1}{2}$ the coefficients $\beta_0 = (1-\varepsilon)\,\alpha$, $\beta_1 = \varepsilon\,\kappa\,\alpha - \frac{1}{2}\,\varepsilon\,(1-\kappa)$, and $\alpha = \frac{\varepsilon}{2}\,(3\,\kappa - 1)\,\alpha$, which gives

$$\kappa^+(\varepsilon) = 1 - \frac{2\,(\alpha - 1)}{3\,\varepsilon\,\alpha},$$
$$\kappa^-(\varepsilon) = \frac{(2-\varepsilon)\,\alpha - 2}{3\,\varepsilon\,\alpha}. \tag{32}$$

Both results are shown in Fig. 4. Without self-feedback ($\kappa = 0$), a bidirectionally coupled pair cannot synchronize, whereas a triangle synchronizes for $\varepsilon > 2\,(\alpha - 1)/\alpha$.

Note that the upper boundaries κ^+ do not depend on the delay time τ, whereas with decreasing delay time the lower boundary moves down and the region of synchronization increases.

From Eq. (24), a relation between the MSF and the maximal Lyapunov exponent in the limit of $\tau \to \infty$ can be derived. We consider a network without self-feedback and with local stability $\beta_0 < 1$. The MSF (i.e., the largest transversal Lyapunov exponent) is given by

$$\lambda = \frac{1}{\tau}\ln\frac{|\sigma_1\,\alpha\,\gamma_1|}{1-\beta_0}, \tag{33}$$

whereas the maximal Lyapunov exponent, which is the Lyapunov exponent parallel to the SM, is

$$\lambda_{\max} = \frac{1}{\tau}\ln\frac{|\sigma_1\,\alpha|}{1-\beta_0}. \tag{34}$$

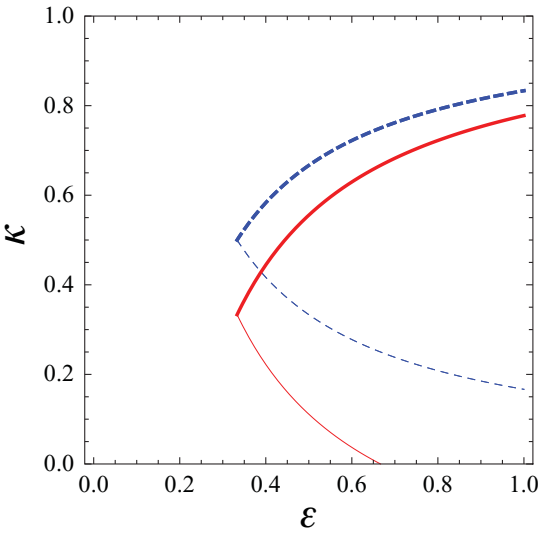

FIG. 4. (Color online) Blue dashed line is the border to synchronization for a bidirectionally coupled Bernoulli pair with $\alpha = 1.5$, self-feedback, $\tau \to \infty$, and ε,κ notation. The thick dashed line denotes κ^+, and the thin line denotes κ^-. Red solid line is the border to synchronization for a bidirectionally coupled triangle, with same parameters as for the pair.

Hence, one obtains

$$\lambda = \lambda_{\max} + \frac{1}{\tau}\ln|\gamma_1|. \tag{35}$$

Thus, the SM is stable if

$$|\gamma_1| < \mathrm{e}^{-\lambda_{\max}\,\tau}, \tag{36}$$

where the product $\lambda_{\max}\,\tau$ is finite for $\tau \to \infty$ if the local Lyapunov exponent is negative. This equation has a fundamental meaning. For any network with a stochastic coupling matrix G, it relates the eigenvalue gap $1 - |\gamma_1|$ to the synchronizability of the network. If the second largest eigenvalue is smaller than the largest one, $|\gamma_1| < 1$, the SM is stable for sufficiently weak chaos inside of the SM, that is, in the limit $\lambda_{\max} \to 0$.

We believe that Eq. (36) holds for any chaotic network of the structure defined in the previous section, even for corresponding delay differential equations. In fact, Eq. (36) has been derived for networks with periodic dynamics [44], and our numerical results of laser equations confirm this condition on chaos synchronization (see the following section).

Equation (36) has been derived in the limit $\tau \to \infty$. For finite τ, one either has to solve Eq. (20) numerically or one can calculate regions of stability with the Schur-Cohn theorem [39]. Even in this case of finite τ, an analytic result is possible. The border of stability is given by $|z_r| = 1$, where $|z_r|$ is the maximal root for the perturbation modes k transversal to the SM. With $z_r = \mathrm{e}^{\mathrm{i}\,\phi_r}$, one can decompose Eq. (20) into the real and imaginary parts:

$$\cos(\phi_r\,\tau) = \beta_0\cos[\phi_r\,(\tau-1)] + \beta_1,$$
$$\sin(\phi_r\,\tau) = \beta_0\sin[\phi_r\,(\tau-1)]. \tag{37}$$

The solution of Eqs. (37) gives boundaries $\beta_1(\phi)$ and $\beta_0(\phi)$. The maximal value of $\beta_0(\phi)$, the tip of the phase diagram of Fig. 3, is obtained in the limit $\phi \to 0$, which gives

$$1 = \beta_0 + \beta_1, \tag{38}$$

$$\tau = \beta_0 (\tau - 1). \tag{39}$$

The first part agrees with Eq. (19), and the second gives the result

$$\max \beta_0 = \frac{\tau}{\tau - 1}. \tag{40}$$

In the limit $\tau \to \infty$, one can synchronize only for $\beta_0 < 1$, that is, if the local Lyapunov exponent (see previous section) is negative. However, for finite delay times even chaotic units ($\beta_0 > 1$) can synchronize if

$$\beta_0 < \frac{\tau}{\tau - 1}. \tag{41}$$

B. Two delay times

Now consider a network with two delay times τ_1 and τ_2 ($\tau_2 > \tau_1$). Each delay time belongs to a coupling matrix G_1 and G_2, which have identical eigenvectors (i.e., identical modes of perturbation). The stability of the SM is determined by the polynomials

$$z^{\tau_2} = \beta_0 z^{\tau_2 - 1} + \beta_1 z^{\tau_2 - \tau_1} + \beta_2. \tag{42}$$

We consider only networks where β_1 and β_2 belong either to a coupling or a self-feedback; therefore we rule out $\eta_i \neq 0$ and $\sigma_i \neq 0$ for the same system. Each mode of perturbation has an eigenvalue $\gamma_{k,l}$ of the coupling matrices of Eq. (1), which gives three possibilities for Eq. (42): a system with self-feedback τ_1 and coupling τ_2, a system with self-feedback τ_2 and coupling τ_1, and a system with two couplings τ_1 and τ_2. For these three cases, we obtain the equations

$$z^{\tau_2} = \eta_0 \alpha z^{\tau_2 - 1} + \eta_1 \alpha z^{\tau_2 - \tau_1} + \sigma_2 \alpha \gamma_{k,2}, \tag{43}$$

$$z^{\tau_2} = \eta_0 \alpha z^{\tau_2 - 1} + \sigma_1 \alpha \gamma_{k,1} z^{\tau_2 - \tau_1} + \eta_2 \alpha, \tag{44}$$

$$z^{\tau_2} = \eta_0 \alpha z^{\tau_2 - 1} + \sigma_2 \alpha \gamma_{k,1} z^{\tau_2 - \tau_1} + \sigma_2 \alpha \gamma_{k,2}. \tag{45}$$

For simplicity, we start the discussion omitting the local term, $\eta_0 = 0$, and considering a pair of coupled units with $\gamma_0 = 1$, $\gamma_1 = -1$. Hence, Eq. (42) is reduced to

$$z^{\tau_2} = \beta_1 z^{\tau_2 - \tau_1} + \beta_2. \tag{46}$$

Let μ be the greatest common divisor of τ_2 and τ_1. We can substitute $w = z^{\mu}$ to obtain

$$w^p = \beta_1 w^{p-q} + \beta_2 \tag{47}$$

with $\tau_2 = p\,\mu$, $\tau_1 = q\,\mu$, and (p,q) are relatively prime. Now, all roots z_r for $k > 0$ lie inside the unit circle if and only if all roots w_r for $k > 0$ lie in the unit circle, and hence only the ratio $\tau_2/\tau_1 = p/q$ determines the stability of Eq. (46). Figure 5 shows the regions of stability of Eq. (46) for different values of p and q calculated with the Schur-Cohn theorem [39]. As shown before, the system is chaotic if $(\eta_1 + \sigma_1)\alpha + (\eta_2 + \sigma_2)\alpha > 1$. For the mode $\gamma_0 = 1$, this means $\beta_1 + \beta_2 > 1$. For example, the point in region I in Fig. 5(a) belongs to a chaotic system.

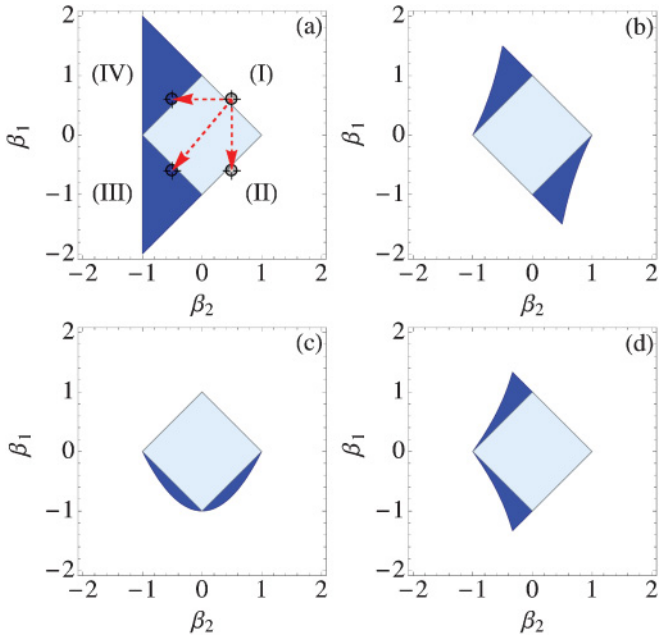

FIG. 5. (Color online) Synchronization regime for $z^{\tau_2} = \beta_1 z^{\tau_2 - \tau_1} + \beta_2$ and $\tau_2/\tau_1 = p/q$ with p,q relatively prime and (a) $\frac{p}{q} = 2$, (b) $\frac{p}{q} = 3$, (c) $\frac{p}{q} = \frac{3}{2}$, and (d) $\frac{p}{q} = 4$. Region I denotes the region parallel to the synchronization manifold, and the other regions are transversal to the synchronization manifold.

The stability of the SM for a bipartite network, for example, a pair of units, is determined by the mode $\gamma_1 = -1$, which changes the sign of β_1 and/or β_2 of the point in region I, depending whether this term belongs to a coupling or to a self-feedback. For self-feedbacks one has $\beta_i = \eta_i \alpha$, whereas the coupling gives $\beta_i = -\sigma_i \alpha$. For example, if τ_1 belongs to a self-feedback, β_1 is positive, since η and α are positive. For τ_2 belonging to a bipartite coupling, G_2 has an eigenvalue $\gamma_1 = -1$, so β_2 is flipped to $-\beta_2$, which gives the point in region IV in Fig. 5(a), which is stable. When both delay times τ_1 and τ_2 belong to the coupling, G_1 and G_2 are coupling matrices with $\gamma_1 = -1$, and we obtain the point in region III which is stable, as well. In both cases, we find complete zero-lag synchronization. However, when τ_2 belongs to a self-feedback and τ_1 to a coupling, we obtain the point in region II, which is unstable. In this case, we can never achieve synchronization for any parameters σ_1 and σ_2 for which the system is chaotic.

Obviously, the symmetries seen in Fig. 5 prevent synchronization for some cases depending on the values of p and q. These symmetries of Eq. (42) can be derived as follows. If we change the sign of the roots, $w = -v$, the conditions of stability do not change, but Eq. (47) is changed to the polynomial

$$v^p = \beta_1 (-1)^q v^{p-q} + \beta_2 (-1)^p. \tag{48}$$

Now, we have to consider three cases:

If q is even and p is odd, the phase diagram has the reflection symmetry $\beta_2 \to -\beta_2$; see Fig. 5(c) for $p = 3$ and $q = 2$. Thus, if τ_1 belongs to the self-feedback and τ_2 to the coupling, the

system cannot synchronize, since the condition for stability of the SM is identical to the condition for chaos.

If q is odd and p is even, the phase diagram has the reflection symmetry $\beta_1 \to -\beta_1$; see Figs. 5(a) and 5(d). Thus, if τ_1 belongs to the coupling and τ_2 to the self-feedback, the system cannot synchronize.

If p as well as q are odd, the phase diagram has the point symmetry $\beta_1 \to -\beta_1$ and $\beta_2 \to -\beta_2$. Thus, if both delay times belong to couplings, the system cannot synchronize.

Therefore, the symmetries of the roots of the polynomials Eq. (46) rule out some ratios of the two delay times for which synchronization can occur. For the ratios which are not forbidden by symmetries, synchronization is possible in a limited paramter region, shown by the dark regions of Fig. 5 for a pair of Bernoulli units. From numerical calculations, we observe that this region shrinks to zero when p and q increase, and we later show that zero-lag synchronization is not possible if τ_1 and τ_2 are large with a small difference.

These results are in agreement with [36,45] where a pair with multiple feedback and multiple couplings with different delay times was analyzed. The time delays which lead to zero-lag synchronization follow [36], Eq. (29)], $\sum_{i=1}^{M_s} l_i\, N_{d_i} + \sum_{j=1}^{M_m} m_j\, N_{c_j} = 0$, where N_{d_i} are the delay times of the M_s different self-feedbacks, N_{c_j} are the delay times of the M_m different couplings, and l_i, m_j are whole numbers with a restricted set of possible values which are specific for each system.

Note, however, that Fig. 5 holds for any network with eigenvalues γ_k. For example, if τ_1 and τ_2 belong to the mutual couplings of a triangle without self-feedback, we have $\gamma_0 = 1$ and $\gamma_{1,2} = -1/2$. Hence, the point in region I of Fig. 5(a) is mapped to $\beta_1 \to -\beta_1/2$ and $\beta_2 \to -\beta_2/2$. This means that the triangle can synchronize for any ratio p,q since the perturbation modes are located in the interior square, which is always stable. This result is due to Gershgorin's circle theorem (15) and the conclusion found earlier in this section. Symmetries rule out synchronization for bipartite networks, only.

Up to now, we have neglected the local term $\eta_0\, \alpha\, z^{\tau_2 - 1}$ in Eq. (42). We show that the symmetries still hold in the limit $\tau_2 \to \infty$, $\tau_1 \to \infty$, $\tau_2/\tau_1 = p/q$. The stability of the SM is determined by the roots of

$$z^{\tau_2} = \eta_0\, \alpha\, z^{\tau_2 - 1} + \beta_1\, z^{\tau_2 - \tau_1} + \beta_2. \tag{49}$$

The border to synchronization is necessarily given by $|z| = 1$, where $|z|$ is the maximum of all roots z_r. With $z = \mathrm{e}^{\mathrm{i}\phi}$, we obtain

$$1 = \eta_0\, \alpha\, \mathrm{e}^{-\mathrm{i}\phi} + \beta_1\, \mathrm{e}^{-\mathrm{i}\phi\, \tau_2\, q/p} + \beta_2\, \mathrm{e}^{-\mathrm{i}\phi\, \tau_2}. \tag{50}$$

In the limit of $\tau_2 \to \infty$, we use the fact that the phases ϕ of the roots are uniformly distributed in $[0,2\pi]$ [42,43]. Hence, there exists one root which is close to $\phi = n\,\pi\,\frac{p}{\tau_2} = n\,\pi\,\frac{q}{\tau_1}$ with some integer n. Following this root in the limit $\tau_2 \to \infty$, we obtain

$$1 = \eta_0\, \alpha + \beta_1\, \mathrm{e}^{-\mathrm{i}n\pi\, q} + \beta_2\, \mathrm{e}^{-\mathrm{i}n\pi\, p}. \tag{51}$$

Now the border to chaos

$$1 = \eta_0\, \alpha + (\eta_1 + \sigma_1)\alpha + (\eta_2 + \sigma_2)\alpha \tag{52}$$

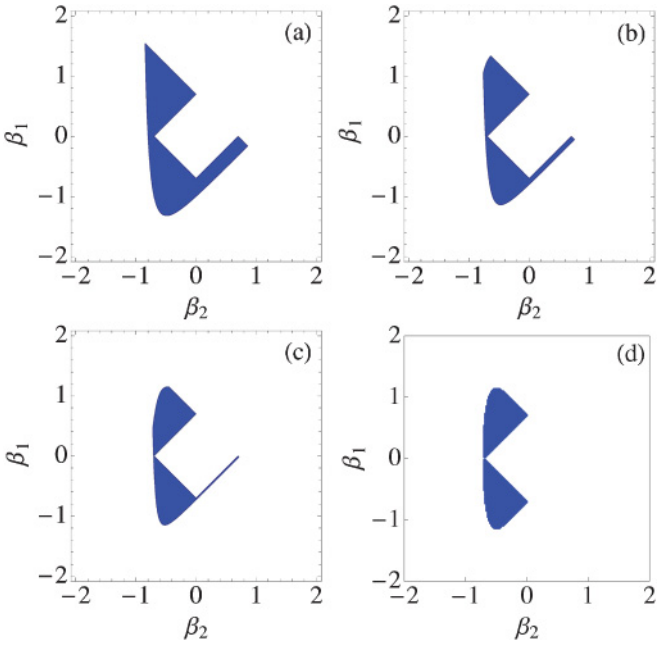

FIG. 6. (Color online) Synchronization regime for $z^{\tau_2} = \beta_0\, z^{\tau_2 - 1} + \beta_1\, z^{\tau_2 - \tau_1} + \beta_2$ and $\tau_2/\tau_1 = 2$ with $\beta_0 = 0.3$. It is (a) $\tau_2 = 4$, (b) $\tau_2 = 8$, (c) $\tau_2 = 16$, and (d) $\tau_2 = 100$. The symmetry found for $\tau_2/\tau_1 = 2$ and $\beta_0 = 0$ is restored for $\beta_0 > 0$ and large values of τ_i.

can be mapped to Eq. (51), depending on whether τ_1 and τ_2 belong to self-feedback or coupling delays. For example, if τ_1 and τ_2 belong to a coupling, Eq. (51) becomes

$$1 = \sigma_0\, \alpha - \sigma_1\, \alpha\, \mathrm{e}^{-\mathrm{i}n\pi\, q} - \sigma_2\, \alpha\, \mathrm{e}^{-\mathrm{i}n\pi\, p}. \tag{53}$$

If both p and q are odd, we choose $\mathrm{e}^{-\mathrm{i}n\pi} = -1$ and Eq. (52). As synchronization regions calculated with the Schur-Cohn theorem show, Eq. (51) is the border to synchronization. Hence, synchronization is not possible. This shows that the ratios $\tau_2/\tau_1 = p/q$ for which synchronization is ruled out by symmetry do not depend on the local term in the limit of large delay times $\tau_i \to \infty$. In fact, the numerical simulations (Fig. 6) show that the symmetries of the complete phase diagram are the same as the ones proven before for $\eta_0 = 0$, although the phase diagram depends on the strength η_0 of the local term.

We have shown that the symmetries of the stability equation, Eq. (49), rule out some ratios of the delay times. In fact, these results support self-consistent arguments for general chaotic networks. These arguments are based on the fact that the information of each trajectory of each unit has to mix after multiples of time intervals τ in order to achieve zero-lag synchronization [23].

Finally, we consider the question to which extent the network is sensitive to detuning the delay times τ_2 and τ_1. It turns out that synchronization is extremely sensitive to a tiny detuning for large delay times. For simplicity, consider the case $\eta_0 = 0$, $\tau_1 = \tau$, $\tau_2 = \tau + \Delta$ with $\tau \to \infty$ where Δ remains finite. τ_1 belongs to a self-feedback, and τ_2 belongs to the coupling of a bipartite network, for example, a pair of Bernoulli units. The boundary to chaos is determined by

$$1 \leqslant \eta_1\, \alpha + \sigma_2\, \alpha, \tag{54}$$

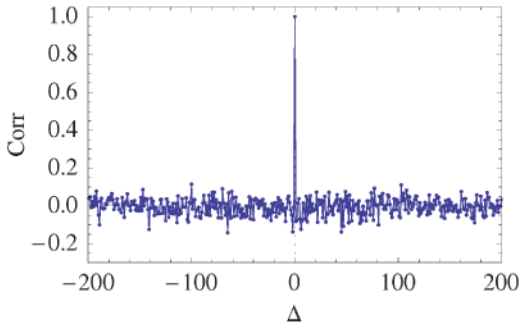

FIG. 7. (Color online) Cross-correlation for a bidirectionally coupled Bernoulli pair with self-feedback delay time τ_1 and coupling delay time $\tau_2 = 10000$. $\Delta = \tau_2 - \tau_1$. The slope $\alpha = 1.1$.

and the stability of the synchronization manifold is given by the polynomial for $\gamma_1 = -1$

$$z^\tau = \eta_1 \alpha z^{-\Delta} - \sigma_2 \alpha. \tag{55}$$

The stability is determined by the largest root $z_k = e^{i\phi} e^{\Lambda/\tau}$, which gives

$$\begin{aligned} e^{2\Lambda} &= |\eta_1 \alpha e^{-i\phi\Delta} - \sigma_2 \alpha|^2 \\ &= (\eta_1 \alpha \cos\phi\,\Delta - \sigma_2 \alpha)^2 + \eta_1^2 \alpha^2 \sin^2\phi\,\Delta \\ &= \eta_1^2 \alpha^2 + \sigma_2^2 \alpha^2 - 2\eta_1 \sigma_2 \alpha^2 \cos\phi\,\Delta. \end{aligned} \tag{56}$$

In the limit $\tau \to \infty$, the distribution of the phase ϕ of the roots is uniform in $[0,2\pi]$, and hence we always find one root with $\cos(\phi\,\Delta) \approx -1$, which according to (54) gives a positive transverse Lyapunov exponent Λ/τ. Thus, even when the self-feedback delay differs from the coupling delay by a single time step, $\tau_2 = \tau_1 \pm 1$, a pair of Bernoulli units cannot synchronize for $\tau_2 \to \infty$. In fact, Fig. 7 shows that the cross-correlation immediately decreases to zero when the delay times are detuned.

C. Multiple delay times

Some of the results of the previous paragraphs can immediately be extended to a network with M delay times [36,45]. In particular, we can rule out complete zero-lag synchronization for some networks in the limit of large delay times.

First, if one delay time is much larger than all other ones, we find the following result: If the network without the long delay does not synchronize, this network cannot be synchronized by adding the long delay.

Second, if for a pair of coupled units all delay times are much larger than the time scales of the isolated units, then synchronization is ruled out for specific ratios of the delay times.

Note that we restrict our discussion to networks defined in the previous section: To each delay time τ_l there exists a coupling matrix G_l with constant row sum, and all matrices G_l have identical eigenvectors with eigenvalues $\gamma_{k,l}$; $k = 0,\ldots,N-1$; $l = 1,\ldots,M$. The stability of the SM is determined by the polynomials

$$z^{\tau_M} = \sum_{l=0}^{M} \beta_l z^{\tau_M - \tau_l}. \tag{57}$$

1. Long delay time τ_M

First we consider a network where the largest delay time τ_M is much larger than all other delays τ_l; that is, we discuss the limit $\tau_M \to \infty$ with finite τ_l, $l \neq M$. Equation (57) can be rewritten as

$$z = \sum_{l=0}^{M-1} \beta_l z^{1-\tau_l} + \beta_M z^{1-\tau_M}. \tag{58}$$

If this equation has a root $|z| > 1$ in the limit of $\tau_M \to \infty$, this root is obviously determined by the first term of Eq. (58). Hence, if the mode k is unstable for the network without long delay, the last term of Eq. (58) cannot stabilize this perturbation. If, however, the largest root of Eq. (58) approaches the unit circle for $\tau_M \to \infty$, the long delay has an influence. We rewrite Eq. (57) as

$$z^{\tau_M} = \frac{\beta_M}{1 - \sum_{l=0}^{M-1} \beta_l z^{-\tau_l}}. \tag{59}$$

In the limit of $\tau_M \to \infty$, we make the ansatz $z = e^{\Lambda/\tau_M} e^{i\phi}$, which gives

$$e^{\Lambda} = \frac{|\beta_M|}{\left|1 - \sum_{l=0}^{M-1} \beta_l z^{-i\phi\tau_l}\right|}. \tag{60}$$

As before, the Lyapunov exponents of the k mode depend only on the modulus of the coupling $\beta_M = (\eta_M + \sigma_M \gamma_{k,M})\alpha$. However, the maximal Lyapunov exponent is not given by $\phi = 0$. Only if all parameters β_l are positive do we obtain the boundary to stability as

$$|\beta_M| = \left|1 - \sum_{l=0}^{M-1} \beta_l\right|. \tag{61}$$

In this case, all β_l belong to self-feedbacks and only β_M is a coupling.

The stability of the SM is determined by negative or complex eigenvalues $\gamma_{k,l}$. For this case, we find an interference of different phases $\phi\tau_l$ in Eq. (60) resulting in a nonobvious value ϕ_0 for the maximal Lyapunov exponent $\lambda_{\max}$. For example, for $\tau_1 = 3$ and $\tau_2 = 300$, we obtain the phase diagram of Fig. 8. This means that a pair of units that is chaotic (cross in Fig. 8) can be synchronized if τ_1 belongs to a coupling and τ_2 to a coupling or a self-feedback. If, however, τ_1 belongs to a self-feedback, τ_2 cannot synchronize this pair. Note that the situation is different for networks with $|\gamma_1| < 1$ (e.g., triangles).

2. Symmetry

Similar to the case of two delay times discussed before, the symmetry of the polynomial Eq. (57) rules out synchronization for a pair of units with specific ratios of the delay times τ_l. This symmetry holds for $\beta_0 = 0$ for general values of τ_l but for $\beta_0 \neq 0$ only if all values of τ_l are large. For simplicity, we discuss the case $\beta_0 = 0$.

First, we consider the greatest common divisor τ of all delay times τ_l; that is, we define $p_l = \tau_l/\tau$ where the integers p_l are

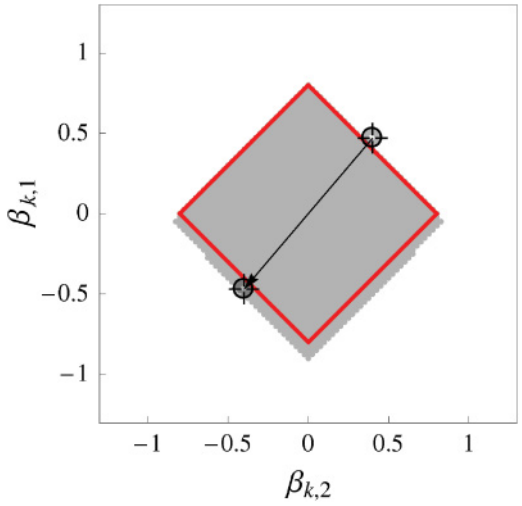

FIG. 8. (Color online) Synchronization area of a system with two time delays $\tau_1 = 3$, $\tau_2 = 300$ and $\beta_0 = 0.2$. The red lines mark the lines $1 - \beta_0 = |\beta_1| + |\beta_2|$. The black crosses exemplify a pair of units which is chaotic and can synchronize if τ_1 belongs to a coupling and τ_2 to a coupling or a self-feedback but not if τ_1 belongs to a self-feedback.

relatively prime. Second, we substitute $w = z^\tau$ in Eq. (57) and obtain

$$w^{p_M} = \sum_{l=0}^{M} \beta_{k,l}\, w^{p_M - p_l}. \tag{62}$$

If a root z_r of Eq. (57) lies inside (outside) the unit circle, the root w_t of Eq. (62) lies inside (outside) as well. Hence, the stability of the perturbation k can be discussed using Eq. (62).

The system is chaotic; Eq. (62) has at least one root $|z_r| > 1$ for $\gamma_0 = 1$, that is, for

$$w^{p_M} = \sum_{l=0}^{M} (\eta_l + \sigma_l)\alpha\, w^{p_M - p_l}. \tag{63}$$

If we restrict our discussion to a pair of units where each τ_l either belongs to a self-feedback $\beta_l = \eta_l\, \alpha$ or a coupling $\beta_l = -\sigma_l\, \alpha$, we can map the stability of the SM to Eq. (63) for specific values of p_l. We find the following result: Synchronization is ruled out if p_l is odd for a coupling and if p_l is even for a self-feedback. These results have been previously seen [36,45]. If synchronization is not ruled out by symmetry, the distinct synchronization area depends on the couplings parameters of the network as well as on the slope of the Bernoulli map.

IV. COMPARISON WITH OTHER SYSTEMS

The analytic results of the previous section were obtained for networks of Bernoulli units. For this case, the linear equations describing the stability of the SM have constant coefficients. This fact allows a stability analysis with polynomials of degree τ_M, the largest delay time.

For networks of general nonlinear units, however, the stability equations have time-dependent coefficients generated by the chaotic trajectory of the SM. For example, for general coupled map lattices, the stability of the SM is determined by Eq. (4), where the time-dependent coefficients are given by the dynamics on the SM, Eq. (2). To our knowledge, these equations cannot be solved analytically. Hence, we compare our analytic calculations of Sec. II with numerical simulations of the skewed tent map

$$f : [0,1] \to [0,1] \quad f(x) = \begin{cases} \frac{x}{a} & \text{if } x \leqslant a, \\ \frac{1-x}{1-a} & \text{if } x > a, \end{cases} \tag{64}$$

with $0 < a < 1$. We choose $a = 0.86$, which results in the same Lyapunov exponent for an isolated unit as the one of the Bernoulli map

$$f : [0,1] \to [0,1], \quad f(x) = \left(\frac{3}{2}\, x\right) \bmod 1. \tag{65}$$

Coupled map lattices are special dynamical systems. Thus, it will be interesting to compare the analytic results of Sec. II with systems of nonlinear differential equations. In particular, we consider the Lang-Kobayashi (LK) equations for coupled semiconductor lasers [23,46]. In some cases, we even compare our results with experiments on chaotic semiconductor lasers.

For networks of differential equations, the mathematical structure corresponding to Eq. (1) is defined by

$$\dot{\vec{x}}_i(t) = \vec{F}[\vec{x}_i(t)] + \sum_{l=1}^{M} \eta_l\, \vec{H}[\vec{x}_i(t - \tau_l)] + \sum_{l=1}^{M} \sum_{j=1}^{N} \sigma_l\, G_{l,ij}\, \vec{H}[\vec{x}_j(t - \tau_l)]. \tag{66}$$

Now $\vec{x}(t)$ is a multidimensional vector. For example, for the LK equations $\vec{x}(t)$ contains the real and imaginary parts of the envelope of the electric field and the population inversion of the charge carriers. Details are given in the Appendix A. The dynamics of the SM is given by

$$\dot{\vec{s}}(t) = \vec{F}[\vec{s}(t)] + \sum_{l=1}^{M} (\eta_l + \sigma_l)\vec{H}[\vec{s}(t - \tau_l)]. \tag{67}$$

The stability of the SM is described by linear equations for each mode k with eigenvalues $\gamma_{k,l}$ of the coupling matrix G_l. The equations corresponding to Eq. (4) are

$$\dot{\vec{\xi}}_k(t) = \mathrm{D}F[\vec{s}(t)]\vec{\xi}_k(t) + \sum_{l=1}^{M} (\eta_l + \sigma_l\, \gamma_{k,l})\mathrm{D}H \times [\vec{s}(t - \tau_l)]\vec{\xi}_k(t - \tau_l) \tag{68}$$

$\mathrm{D}F$ and $\mathrm{D}H$ are the Jacobian matrices of $\vec{F}$ and $\vec{H}$ respectively evaluated at the SM. The MSF for the LK equations is defined in the Appendix A. In the following paragraphs, we consider networks with a single delay time, $M = 1$, and with double delays, $M = 2$.

A. Networks with a single delay time

In the previous section, we obtained the analytic result that the eigenvalue gap of the coupling matrix determines the stability of the SM in the limit of large delay times τ, which will be realized in this section by $\tau = 100$ ns for the LK equations and $\tau = 100$ for the tent map and the Bernoulli map. The relation $|\gamma_1| < \exp(-\lambda_{\max}\, \tau)$ of Eq. (36) is the condition

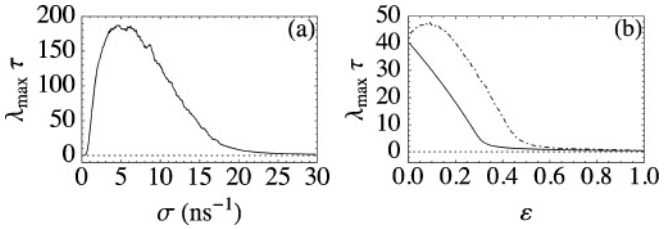

FIG. 9. Maximal Lyapunov exponents of the synchronization manifold for a network of (a) lasers modeled by LK equations and (b) tent maps (dot-dashed line) and Bernoulli maps (solid line).

for a stable SM; it relates the maximal Lyapunov exponent $\lambda_{\max}$ of the SM to the second largest modulus of the eigenvalues of the coupling matrix G.

As a consequence of Eq. (36), a pair of units without self-feedback cannot be synchronized, since $\gamma_1 = -1$. This result agrees with experiments on semiconductor lasers [47]. Two lasers coupled by their mutual laser beams cannot be synchronized with zero time lag; only high correlations with a time shift of τ have been observed.

With self-feedback, however, the situation is different. Equations (26) and (31) show that a pair of units can be synchronized if the local Lyapunov exponent is negative. Again, this result agrees with experiments on semiconductor lasers where the self-feedback is realized by external mirrors [48–53].

Thus, qualitatively, the relation Eq. (36) is in agreement with experiments on lasers. Unfortunately, up to now, experiments on larger networks of coupled lasers are not reported. Hence, the quantitative comparison with lasers has to rely on numerical simulations of the LK equations.

Figure 9 shows the numerically calculated maximal Lyapunov exponent $\lambda_{\max}$ as a function of the coupling parameter σ for a network of lasers and as a function of the coupling parameter ε for a network of tent maps and Bernoulli maps. Self-feedback is suppressed ($\eta = 0$). The parameters for the LK equations are defined in the Appendix A.

For a triangle with bidirectional couplings, it is $\gamma_1 = -\frac{1}{2}$. Equation (36) predicts a transition to synchronization for $\lambda_{\max}\,\tau = -\ln(\frac{1}{2}) \approx 0.69$, the horizontal dashed line in Fig. 10(a). The numerical results of Fig. 10 give a critical coupling $\varepsilon_c \approx 0.9$ for the tent maps [vertical dashed line in Fig. 10(b)] and two critical couplings $\sigma_{c,1} \approx 0.45\,\mathrm{ns}^{-1}$ and $\sigma_{c,2} \approx 45\,\mathrm{ns}^{-1}$ for the three lasers [vertical dashed line in

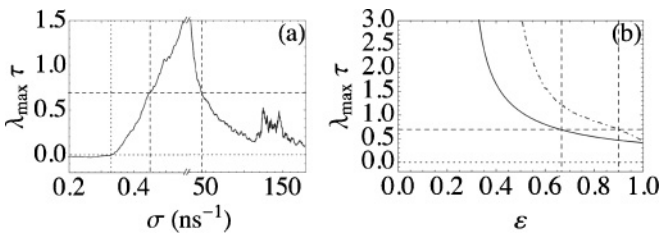

FIG. 10. Enlarged view of Fig. 9, the critical coupling strengths (dashed lines) according to Eq. (36), for the synchronization of a triangle of (a) lasers modeled by LK equations and (b) tent maps (dot-dashed line) and Bernoulli maps (solid line) without self-feedback.

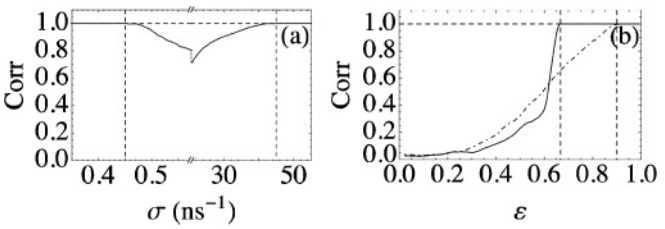

FIG. 11. Critical coupling strengths (dashed lines) for synchronization measured in numerical simulations of a triangle of (a) lasers modeled by LK equations and (b) tent maps (dot-dashed line) and Bernoulli maps (solid line) without self-feedback.

Fig. 10(a)]. Figure 11 shows the cross-correlations obtained from numerical simulations of the corresponding triangle. We find the measured critical couplings of the tent maps and the LK equations to be in good agreement with the predictions of Eq. (36).

A more challenging test of the condition Eq. (36) is a network with directed couplings. In this case, the eigenvalue γ_1 is a complex number. For example, for the square with one diagonal of Fig. 1, one can add an additional coupling strength ρ for the diagonal and obtain the eigenvalue gap of Fig. 12. The largest gap is obtained for $\rho = \frac{5}{8}$ with $\gamma_1 = \frac{-1 \pm i\sqrt{11}}{4}$.

Combining this result with Eq. (36) and $\lambda_{\max}(\sigma)$ [Fig. 9(a)], we obtain the phase diagram of Fig. 13 for the corresponding laser network. Figure 13 also shows parameters for which complete zero-lag synchronization is achieved in numerical simulations of the complete laser network. We define complete zero-lag synchronization between the lasers for isochronal cross-correlations larger than 0.99 in between the power dropouts of the low-frequency fluctuations, which happen on a time scale of the order of magnitude of $10\,\tau$. While it makes sense to speak of complete synchronization for such values of the cross-correlations, the maximal Lyapunov exponent is still slightly positive for correlations around 0.99. Hence, some of the shown points of complete synchronization in Fig. 13 lie outside of the predicted stability border, which corresponds to a maximal Lyapunov exponent of exactly zero. The quantitative agreement between the relation Eq. (36) and the phase diagram Fig. 13 of complete zero-lag synchronization is remarkable.

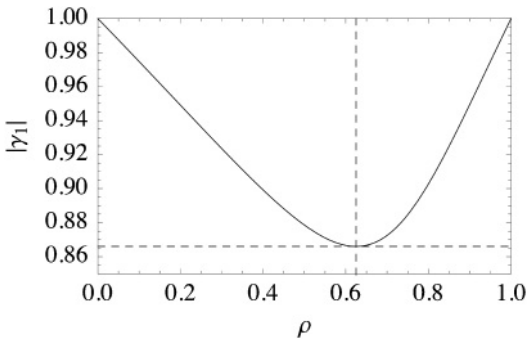

FIG. 12. Eigenvalue $|\gamma_1|(\rho)$ for the square with directed couplings and one diagonal with coupling strength ρ. The dashed line indicates the position of the largest eigenvalue gap.

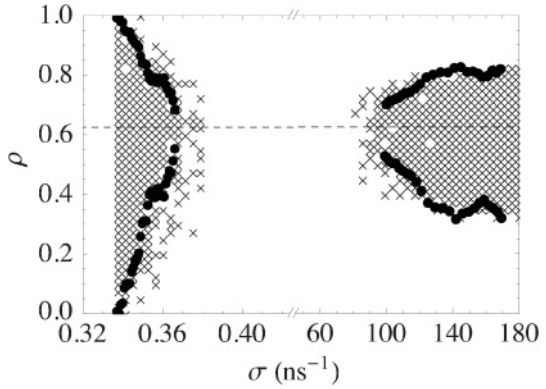

FIG. 13. Phase diagram for a square of lasers with directed couplings and one diagonal with coupling strength ρ. The crosses denote parameters for which complete zero-lag synchronization is achieved in numerical simulations (only synchronization for chaotic dynamics on the SM is shown), the dots indicate the prediction of the stability border for synchronization, and the dashed line shows the position of the largest eigenvalue gap.

B. Networks with two delay times

A pair of units without self-feedback cannot be synchronized if its coupling has a single delay time. In the previous section, however, we have shown in agreement with [36,45] that zero-lag synchronization is possible if the coupling contains two delay times τ_1 and τ_2. Only if the ratio $\frac{\tau_2}{\tau_1}$ is a ratio of odd relatively prime integers, $\frac{\tau_2}{\tau_1} = \frac{p}{q}$, is synchronization excluded. The parameter region of synchronization is largest for small values of p and q.

This result is in agreement with recent experiments on semiconductor lasers [54]. For $\frac{\tau_2}{\tau_1} = \frac{2}{1}$, complete synchronization was observed. Cross-correlations were large for $\frac{\tau_2}{\tau_1} \in \{\frac{5}{4}, \frac{4}{3}, \frac{3}{2}, \frac{5}{2}\}$ and low for $\frac{\tau_2}{\tau_1} \in \{\frac{1}{1}, \frac{5}{3}, \frac{3}{1}\}$.

The analytic result was based on the symmetry of the phase diagrams, Figs. 5 and 6. Here we show that these symmetries can be observed for the MSF of laser networks and tent maps as well. With two delays, Eqs. (67) and (68) reduce to

$$\dot{\vec{s}}(t) = \vec{F}[\vec{s}(t)] + \sigma_1 \vec{H}[\vec{s}(t-\tau_1)] + \sigma_2 \vec{H}[\vec{s}(t-\tau_2)], \quad (69)$$

$$\begin{aligned}\dot{\vec{\xi}}_k(t) = {} & \mathrm{D}F[\vec{s}(t)]\vec{\xi}_k(t) \\ & + \sigma_1 \gamma_{k,1} \mathrm{D}H[\vec{s}(t-\tau_1)]\vec{\xi}_k(t-\tau_1) \\ & + \sigma_2 \gamma_{k,2} \mathrm{D}H[\vec{s}(t-\tau_2)]\vec{\xi}_k(t-\tau_2). \end{aligned} \quad (70)$$

Because of the invasive nature of the coupling, we obtain a different trajectory $\vec{s}(t)$ on the SM for each pair of coupling strengths (σ_1,σ_2), which in each case gives a different linear stability equation. In order to compare these with the previous section, we fix σ_1 and σ_2, vary $\gamma_{k,1}$ and $\gamma_{k,2}$, and calculate the maximal Lyapunov exponent of the linear equation (70). In this interpretation of $\beta_1 = \sigma_1 \gamma_{k,1}$ and $\beta_2 = \sigma_2 \gamma_{k,2}$, the results are universal in view of the fact that they make a statement about the stability of all modes of every possible network with real $\gamma_{k,1}$ and $\gamma_{k,2}$ for the chosen coupling strengths (σ_1,σ_2). The point $\gamma_{0,1} = \gamma_{0,2} = 1$ is shared among all networks; it determines the stability of the dynamics on the SM.

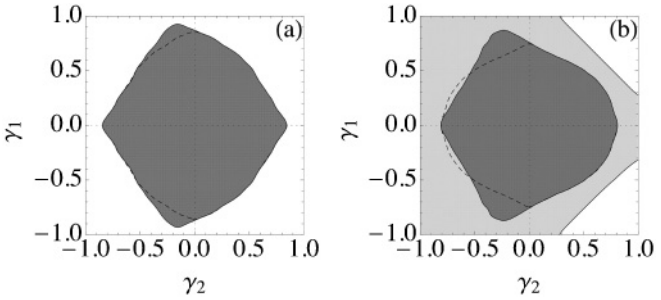

FIG. 14. Region of stability (dark gray regime) for a pair of (a) lasers modeled by the LK equations and (b) tent maps in comparison with a pair of Bernoulli maps (light gray regime) with two coupling delay times, τ_1 and τ_2 and $\frac{\tau_2}{\tau_1} = \frac{2}{1}$. The dashed line indicates reflection of the top right quadrant's stability border into the other quadrants.

Figure 14 shows the results of the numerical simulations of Eqs. (69) and (70) with $\tau_1 = 20\,\mathrm{ns}$, $\tau_2 = 40\,\mathrm{ns}$, and $\sigma_1 = \sigma_2 = 45\,\mathrm{ns}^{-1}$ for the LK equations and $\tau_1 = 200$, $\tau_2 = 400$, $\varepsilon = 0.9$, and $\kappa = 0.5$ for the tent map and the Bernoulli map. As shown in the previous section, the region of stability should have reflection symmetry at the horizontal axis. The stability region for laser networks [Fig. 14(a)] is in agreement with this symmetry. The corresponding stability regions of the networks of tent maps and Bernoulli maps [Fig. 14(b)], coupled with two delay times, show this reflection symmetry as well.

In the previous section, we showed that synchronization is sensitive to detuning of the ratio of the delay times; see Fig. 7. Figure 15 shows that synchronization of two lasers is destroyed if τ_1 and τ_2 differ by about 10 ps, which corresponds to the coherence length of the chaotic lasers. The coupling has a fixed delay time of $\tau_2 = 100\,\mathrm{ns}$ and a strength of $\sigma_2 = 20\,\mathrm{ns}^{-1}$. The self-feedbacks have a delay time of $\tau_1 = \tau_2 + \Delta$ and a strength of $\sigma_2 = 30\,\mathrm{ns}^{-1}$. Thus, in agreement with the analytic results for Bernoulli networks, lasers are sensitive to detuning of the delay times as well [49,50,55]. Of course, the detailed structure of the cross-correlations of Fig. 15 depends on the details of the laser dynamics, which cannot be predicted by iterated maps.

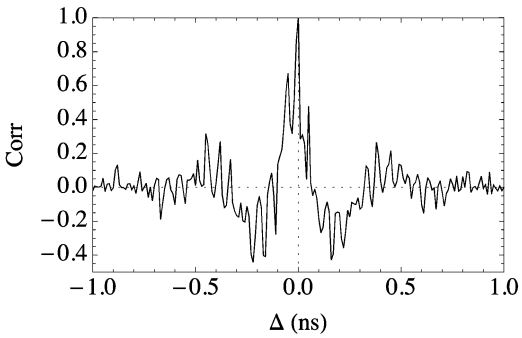

FIG. 15. Sensitivity of cross-correlations to detuning of the delay times τ_2 and $\tau_1 = \tau_2 + \Delta$ for a pair of LK equations.

V. SUMMARY

Chaos synchronization of networks of identical nonlinear units with time-delayed couplings is investigated. Although the units are coupled with long delay times, they synchronize to a common chaotic trajectory without time shift. For rather general networks with multiple delay times, the method of the MSF allows us to relate the stability of the SM to the eigenvalue gaps of the coupling matrices.

For networks of iterated Bernoulli maps, the stability of the SM is calculated analytically in the limit of large delay times. The theory of polynomials allows us to calculate phase diagrams of chaos synchronization and to derive their symmetries. Finally, these analytic results are compared with numerical simulations of iterated tent maps and rate equations for semiconductor lasers (LK equations). Some results can even be compared with recent experiments on semiconductor lasers.

For a single delay time, Eq. (36) is the most important result. It relates the eigenvalue gap of the coupling matrix of the whole network to the Lyapunov exponent of the trajectory of a single unit with feedback. It is exact for Bernoulli networks with a long delay time, but it compares well with our numerical results for networks of tent maps and LK units, too. Even the phase diagram of a directed network with complex eigenvalues, which has been calculated for lasers, is in good agreement with this fundamental equation. For a pair of units without self-feedback and for any bipartite network, the eigenvalue gap is zero, and hence these networks cannot synchronize completely in the limit of a large delay time. Only cluster synchronization is possible.

For networks with several delay times, we could not find a simple relation for the stability of the SM. However, the theory of polynomials showed some symmetries of the phase diagrams for Bernoulli networks. Our numerical results for tent maps and LK equations showed these symmetries, as well. For a pair of units coupled by multiple delay times, these symmetries have interesting consequences. Only for special ratios of the delay times is synchronization possible in the limit of long delay times, in agreement with self-consistent arguments related to mixing of information [23]. Again, this analytic result is in agreement with numerical simulations of the LK equations and even with experiments on semiconductor lasers [54].

These results show that networks of iterated Bernoulli units have universal properties. On the one hand, we have analytic tools to calculate the stability of chaos synchronization since the linearized equations do not contain the chaotic trajectory. On the other hand, we have either numerical simulations of the linearized difference/differential equations containing the chaotic trajectory as input or we have direct simulations of the complete network. We have found that there is good agreement between these different systems, sometimes even on a quantitative level.

ACKNOWLEDGMENTS

We thank the Deutsche Forschungsgemeinschaft and the Leibniz-Rechenzentrum in Garching, Germany, for their support of this work.

TABLE I. Used constants in the simulation of the LK equations. Values are taken from [56].

Parameter	Symbol	Value
Linewidth enhancement factor	α	5
Differential optical gain	G_N	$2.142 \times 10^4\ \mathrm{s}^{-1}$
Laser frequency	ω_0	$\frac{2\pi c}{635\ \mathrm{nm}}$
Pump current relative to J_{th}	p	1.02
Threshold pump current of solitary laser	J_{th}	γN_{sol}
Carrier decay rate	γ	$0.909 \times 10^9\ \mathrm{s}^{-1}$
Carrier number of solitary laser	N_{sol}	1.707×10^8
Cavity decay rate	Γ	$0.357 \times 10^{12}\ \mathrm{s}^{-1}$

APPENDIX A:THE LANG-KOBAYASHI EQUATIONS AND THEIR MASTER STABILITY EQUATIONS

The LK equations in their complex form are

$$\dot{\mathcal{E}}^i(t) = \frac{1+\mathrm{i}\,\alpha}{2} G_N\, n^i(t)\mathcal{E}^i(t) + \sigma_1\, \mathcal{E}^i(t-\tau_1)\mathrm{e}^{-\mathrm{i}\,\omega_0\,\tau_1} + \sigma_2 \sum_{j=1}^{N} G_{ij}\, \mathcal{E}^j(t-\tau_2)\mathrm{e}^{-\mathrm{i}\,\omega_0\,\tau_2}, \tag{A1}$$

$$\dot{n}^i(t) = (p-1)J_{th} - \gamma\, n^i(t) - [\Gamma + G_N\, n^i(t)]|\mathcal{E}^i(t)|^2, \tag{A2}$$

where $\mathcal{E}^i(t)$ is the envelope of the complex electric field and $n^i(t)$ is the renormalized population inversion of the charge carriers of laser i. The constants used are listed in Table I.

For the numerical simulation of the equations, we make the ansatz

$$\mathcal{E}^i(t) = \mathcal{R}^i(t) + \mathrm{i}\,\mathcal{I}^i(t) \tag{A3}$$

and thus obtain the real-valued differential equation system

$$\dot{\mathcal{R}}^i(t) = \frac{1}{2} G_N\, n^i(t)[\mathcal{R}^i(t) - \alpha\mathcal{I}^i(t)] + \sigma_1 \mathcal{R}^i(t-\tau_1)\cos(\omega\,\tau_1) + \sigma_1\, \mathcal{I}^i(t-\tau_1)\sin(\omega\,\tau_1) + \sigma_2 \sum_{j=1}^{N} G_{ij}\, \mathcal{R}^j(t-\tau_2) \times \cos(\omega\tau_2) + \sigma_2 \sum_{j=1}^{N} G_{ij}\mathcal{I}^j(t-\tau_2)\sin(\omega\tau_2), \tag{A4}$$

$$\dot{\mathcal{I}}^i(t) = \frac{1}{2} G_N n^i(t)[\mathcal{I}^i(t) + \alpha\mathcal{R}^i(t)] - \sigma_1\, \mathcal{R}^i(t-\tau_1) \times \sin(\omega\tau_1) + \sigma_1\, \mathcal{I}^i(t-\tau_1)\cos(\omega\,\tau_1) - \sigma_2 \sum_{j=1}^{N} G_{ij}\, \mathcal{R}^j \times (t-\tau_2)\sin(\omega\,\tau_2) + \sigma_2 \sum_{j=1}^{N} G_{ij}\, \mathcal{I}^j(t-\tau_2)\cos(\omega\,\tau_2), \tag{A5}$$

$$\dot{n}^i(t) = (p-1)J_{th} - \gamma\, n^i(t) - [\Gamma + G_N\, n^i(t)]\{[\mathcal{R}^i(t)]^2 + [\mathcal{I}^i(t)]^2\}. \tag{A6}$$

We integrate this differential equation system numerically using Heun's method [57], which is a numerical integration method of the class of Runge-Kutta methods that is particularly suitable for delay-differential equation systems. The used step size for integration is $\Delta t = 0.1$ ps. In order to emulate

the measurement of cross-correlations with a gigahertz oscilloscope in an experimental setup, on the one hand, we define cross-correlations between two simulated lasers as the cross-correlations between the absolute values of their electric fields. On the other hand, we use a sampling time of 1 ns per data point during which the absolute values of the electric field are averaged. For the precision measurement of the sensitivity of cross-correlations to detuning the delay times in Fig. 15, we use a sampling time of 10 ps. Desynchronization of the simulated lasers occurs during the power dropouts of the low-frequency fluctuations, which happen on a time scale of the order of magnitude of $10\,\tau$. In order to avoid measuring cross-correlations during them, the cross-correlations are calculated ten times from comparatively short time windows of the length of $5\,\tau$, and then the five largest cross-correlations are averaged.

The master stability equations of the LK equations are

$$\begin{aligned}\dot{\delta}_{\mathcal{R}}(t) = {} & \tfrac{1}{2} G_{\mathrm{N}} n(t)[\delta_{\mathcal{R}}(t) - \alpha\delta_{\mathcal{I}}(t)] + \tfrac{1}{2} G_{\mathrm{N}}\,\delta_n(t)[\mathcal{R}(t) - \alpha\,\mathcal{I}(t)] \\ & + \sigma_1\,\delta_{\mathcal{R}}(t-\tau_1)\cos(\omega\,\tau_1) + \sigma_1\,\delta_{\mathcal{I}}(t-\tau_1)\sin(\omega\,\tau_1) \\ & + \sigma_2\,\gamma_k\,\delta_{\mathcal{R}}(t-\tau_2)\cos(\omega\tau_2) + \sigma_2\,\gamma_k\,\delta_{\mathcal{I}}(t-\tau_2)\sin(\omega\,\tau_2),\end{aligned} \tag{A7}$$

$$\begin{aligned}\dot{\delta}_{\mathcal{I}}(t) = {} & \tfrac{1}{2}\,G_{\mathrm{N}}\,n(t)[\delta_{\mathcal{I}}(t) + \alpha\delta_{\mathcal{R}}(t)] + \tfrac{1}{2}\,G_{\mathrm{N}}\,\delta_n(t)[\mathcal{I}(t) + \alpha\,\mathcal{R}(t)] \\ & - \sigma_1\,\delta_{\mathcal{R}}(t-\tau_1)\sin(\omega\,\tau_1) + \sigma_1\,\delta_{\mathcal{I}}(t-\tau_1)\cos(\omega\,\tau_1) \\ & - \sigma_2\gamma_k\delta_{\mathcal{R}}(t-\tau_2)\sin(\omega\tau_2) + \sigma_2\gamma_k\delta_{\mathcal{I}}(t-\tau_2)\cos(\omega\tau_2),\end{aligned} \tag{A8}$$

$$\begin{aligned}\dot{\delta}_n(t) = {} & -(\gamma + G_{\mathrm{N}}\{[\mathcal{R}(t)]^2 + [\mathcal{I}(t)]^2\})\delta_n(t) \\ & -2[\Gamma + G_{\mathrm{N}}\,n(t)][\mathcal{R}(t)\delta_{\mathcal{R}}(t) + \mathcal{I}(t)\delta_{\mathcal{I}}(t)],\end{aligned} \tag{A9}$$

which are integrated numerically using Heun's method, as well. We calculate the maximal Lyapunov exponent using Farmer's method [41]. For correspondence to our definition of the cross-correlation above, we define the deviation of the absolute value of the electric field as the metric of the separation function. This is legitimate as the LK equations form a strongly coupled differential equation system.

APPENDIX B:THE SCHUR-COHN THEOREM

In order to find the synchronization areas in parameter space, the Schur-Cohn theorem is a possible method; see [39].The synchronization area for a network of iterated one-dimensional maps with constant slope is derived by finding the parameters for which the roots of the characteristic polynomial lie inside the unit circle.

For a polynomial with $P(x) = \sum_{i=0}^{n} a_i\,x^i$, the Schur-Cohn theorem defines determinants

$$\delta_{\nu+1} = \begin{vmatrix} a_n & 0 & \dots & 0 & a_0 & a_1 & \dots & a_\nu \\ a_{n-1} & a_n & \dots & 0 & 0 & a_0 & \dots & a_{\nu-1} \\ \dots & \dots & \dots & \dots & \dots & \dots & \dots & \dots \\ a_{n-\nu} & a_{n-\nu+1} & \dots & a_n & 0 & 0 & \dots & a_0 \\ \overline{a_0} & 0 & \dots & 0 & \overline{a_n} & \overline{a_{n-1}} & \dots & \overline{a_{n-\nu}} \\ \overline{a_1} & \overline{a_0} & \dots & 0 & 0 & \overline{a_n} & \dots & \overline{a_{n-\nu+1}} \\ \dots & \dots & \dots & \dots & \dots & \dots & \dots & \dots \\ \overline{a_\nu} & \overline{a_{\nu-1}} & \dots & \overline{a_0} & 0 & 0 & \dots & \overline{a_n} \end{vmatrix} \tag{B1}$$

with $\nu = 0, 1, \dots, n-1$.

Due to the Schur-Cohn theorem, it is $|x| < 1$ when all determinants are greater than 0.

[1] A. Pikovsky, M. Rosenblum, and J. Kurths, *Synchronization: A Universal Concept in Nonlinear Sciences* (Cambridge University Press, Cambridge, 2001).

[2] S. Boccaletti, J. Kurths, G. Osipov, D. L. Valladares, and C. S. Zhou, Phys. Rep. **366**, 1 (2002).

[3] A. Balanov, N. Janson, D. Postnov, and O. Sosnovtseva, *Synchronization: From Simple to Complex* (Springer, Berlin, 2009).

[4] E. Mosekilde, Y. Maistrenko, and D. Postnov, *Chaotic Synchronization: Application to Living Systems* (World Scientific, Singapore, 2002).

[5] E. Schöll and H. G. Schuster, eds., *Handbook of Chaos Control* (Wiley-VCH, Weinheim, 2008).

[6] C. W. Wu, *Synchronization in Complex Networks of Nonlinear Dynamical Systems* (World Scientific, Singapore, 2007).

[7] A. Arenas, A. Díaz-Guilera, J. Kurths, Y. Moreno, and C. Zhou, Phys. Rep. **469**, 93 (2008).

[8] P. Colet and R. Roy, Opt. Lett. **19**, 2056 (1994).

[9] A. Uchida, F. Rogister, J. Garcfa-Ojalvo, and R. Roy, Prog. Opt. **48**, 203 (2005).

[10] G. D. VanWiggeren and R. Roy, Science **279**, 1198 (1998).

[11] A. Argyris, D. Syvridis, L. Larger, V. Annovazzi-Lodi, P. Colet, I. Fischer, J. García-Ojalvo, C. R. Mirasso, L. Pesquera, and K. A. Shore, Nature (London) **437**, 343 (2005).

[12] F. M. Atay and T. Bıyıkoğlu, Phys. Rev. E **72**, 016217 (2005).

[13] S.-J. Baek and E. Ott, Phys. Rev. E **69**, 066210 (2004).

[14] M. Barahona and L. M. Pecora, Phys. Rev. Lett. **89**, 054101 (2002).

[15] J. Jost and M. P. Joy, Phys. Rev. E **65**, 016201 (2001).

[16] C. Li, W. Sun, and J. Kurths, Phys. Rev. E **76**, 046204 (2007).

[17] L. M. Pecora and T. L. Carroll, Phys. Rev. Lett. **64**, 821 (1990).

[18] F. S. de San Roman, S. Boccaletti, D. Maza, and H. Mancini, Phys. Rev. Lett. **81**, 3639 (1998).

[19] F. M. Atay, J. Jost, and A. Wende, Phys. Rev. Lett. **92**, 144101 (2004).

[20] C. U. Choe, T. Dahms, P. Hövel, and E. Schöll, Phys. Rev. E **81**, 025205 (2010).

[21] M. G. Earl and S. H. Strogatz, Phys. Rev. E **67**, 036204 (2003).

[22] P. Hövel, M. A. Dahlem, and E. Schöll, Int. J. Bifurcation Chaos Appl. Sci. Eng. **20**, 813 (2010).

[23] I. Kanter, M. Zigzag, A. Englert, F. Geissler, and W. Kinzel, EPL **93**, 60003 (2001).

[24] J. Kestler, W. Kinzel, and I. Kanter, Phys. Rev. E **76**, 035202 (2007).

[25] W. Kinzel, A. Englert, G. Reents, M. Zigzag, and I. Kanter, Phys. Rev. E **79**, 056207 (2009).

[26] G. Kozyreff, A. G. Vladimirov, and P. Mandel, Phys. Rev. Lett. **85**, 3809 (2000).

[27] C. Masoller and A. C. Marti, Phys. Rev. Lett. **94**, 134102 (2005).
[28] B. Schmitzer, W. Kinzel, and I. Kanter, Phys. Rev. E **80**, 047203 (2009).
[29] L. M. Pecora and T. L. Carroll, Phys. Rev. Lett. **80**, 2109 (1998).
[30] V. Flunkert, S. Yanchuk, T. Dahms, E. Schöll, Phys. Rev. Lett. **105**, 254101 (2010).
[31] J. Kestler, E. Kopelowitz, I. Kanter, and W. Kinzel, Phys. Rev. E **77**, 046209 (2008).
[32] I. Kanter, E. Kopelowitz, R. Vardi, M. Zigzag, W. Kinzel, M. Abeles, and D. Cohen, EPL **93**, 66001 (2011).
[33] M. Dhamala, V. K. Jirsa, and M. Ding, Phys. Rev. Lett. **92**, 074104 (2004).
[34] E. M. Shahverdiev and K. A. Shore, Phys. Rev. E **77**, 057201 (2008).
[35] W. Just, E. Reibold, H. Benner, K. Kacperski, P. Fronczak, and J. Hołyst, Phys. Lett. A **254**, 158 (1999).
[36] M. Zigzag, M. Butkovski, A. Englert, W. Kinzel, and I. Kanter, Phys. Rev. E **81**, 036215 (2010).
[37] A. Berman and R. Plemmons, *Nonnegative Matrices in the Mathematical Sciences* (Academic Press, New York, 1979).
[38] S. Gershgorin, Bulletin de l'acad/'emie des Sciences de l'URSS. Classe des sciences mathematiques et na **6**, 749 (1931).
[39] I. Schur, J. Math. **148**, 205 (1917).
[40] S. Lepri, G. Giacomelli, A. Politi, and F. T. Arecchi, Physica D **70**, 235 (1994).
[41] J. D. Farmer, Physica D **4**, 366 (1982).
[42] P. Erdös and P. Turan, Ann. Math. **51**, 105 (1950).
[43] A. Granville, in *Equidistribution in Number Theory: An Introduction*, edited by A. Granville and Z. Rudnick (Springer, the Netherlands, 2007).
[44] S. Yanchuk and P. Perlikowski, Phys. Rev. E **79**, 046221 (2009).
[45] M. Zigzag, M. Butkowski, A. Englert, W. Kinzel, and I. Kanter, Europhys. Lett. **85**, 60005 (2009).
[46] R. Lang and K. Kobayashi, IEEE J. Quantum Electron. **16**, 347 (1980).
[47] I. Fischer, R. Vicente, J. M. Buldu, M. Peil, C. R. Mirasso, M. C. Torrent, and J. García-Ojalvo, Phys. Rev. Lett. **97**, 123902 (2006).
[48] M. Rosenbluh, Y. Aviad, E. Cohen, L. Khaykovich, W. Kinzel, E. Kopelowitz, P. Yoskovits, and I. Kanter, Phys. Rev. E **76**, 046207 (2007).
[49] E. Klein, N. Gross, M. Rosenbluh, W. Kinzel, L. Khaykovich, and I. Kanter, Phys. Rev. E **73**, 066214 (2006).
[50] N. Gross, W. Kinzel, I. Kanter, M. Rosenbluh, and L. Khaykovich, Opt. Commun. **267**, 464 (2006).
[51] E. Klein, N. Gross, E. Kopelowitz, M. Rosenbluh, L. Khaykovich, W. Kinzel, and I. Kanter, Phys. Rev. E **74**, 046201 (2006).
[52] I. Kanter, N. Gross, E. Klein, E. Kopelowitz, P. Yoskovits, L. Khaykovich, W. Kinzel, and M. Rosenbluh, Phys. Rev. Lett. **98**, 154101 (2007).
[53] I. Kanter, M. Butkovski, Y. Peleg, M. Zigzag, Y. Aviad, I. Reidler, M. Rosenbluh, and W. Kinzel, Opt. Express **18**, 18292 (2010).
[54] A. Englert, W. Kinzel, Y. Aviad, M. Butkovski, I. Reidler, M. Zigzag, I. Kanter, and M. Rosenbluh, Phys. Rev. Lett. **104**, 114102 (2010).
[55] Y. Aviad, I. Reidler, W. Kinzel, I. Kanter, and M. Rosenbluh, Phys. Rev. E **78**, 025204 (2008).
[56] V. Ahlers, U. Parlitz, and W. Lauterborn, Phys. Rev. E **58**, 7208 (1998).
[57] K. Heun, Z. Math. Phys **45**, 23 (1900).